Regulation of synoptic circulation in regional PM2.5 transport for heavy air pollution: study of 5-year observation over central China

Weiyang Hu[1], Tianliang Zhao[1], Yongqing Bai[2], Shaofei Kong[3], Lijuan Shen[4], Jie Xiong[5], Yue Zhou[6], Yao Gu[7], Junnan Shi[8], Huang Zheng[3], and Xiao Yun Sun[4]

[1]Nanjing University of Information Science & Technology
[2]Institute of Heavy Rain, China Meteorological Administration
[3]China University of Geosciences (Wuhan)
[4]Nanjing University of Information Science and Technology
[5]Wuhan Institute of Heavy Rain
[6]Wuhan Regional Climate Center
[7]Nanjing University of Information Science &Technology
[8]Taishan meteorological station of Shandong province

November 24, 2022

Abstract

The importance of regional air pollutant transport modulated by large-scale synoptic circulation has been poorly understood for air pollution. In the present study of 5-year (2015-2019) observation, we targeted the Twain-Hu Basin (THB), a region of heavy $PM_{2.5}$ pollution over central China to investigate the regulation of synoptic circulation governing regional $PM_{2.5}$ transport for heavy air pollution. It was found that regional transport of $PM_{2.5}$ predominated 65.2% of the heavy pollution events (HPEs) over the THB based on the statistics of observational environment and meteorology. By employing the FLEXPART-WRF model, the regional transport of $PM_{2.5}$ from upwind source areas in central and eastern China (CEC) to receptor region in the THB was identified with three prominent pathways in the northerly, northeasterly, and easterly directions respectively. Based on T-mode principal component analysis in conjunction with the K-means cluster method, it was recognized that three regional $PM_{2.5}$ transport pathways for the HPEs over central China were determined respectively by three patterns of synoptic circulation over CEC with 1) weak high air pressure to the north, 2) strong high air pressure to the northeast, and 3) weak high air pressure to the east, governing the cold air invasions southwards to the THB region in central China with the large contributions of 76.0%, 56.7%, and 53.9% to the THB- $PM_{2.5}$ concentrations in the HPEs, revealing a significant modulation of large-scale synoptic circulation for regional transport of air pollutants in environmental change.

Regulation of synoptic circulation in regional $PM_{2.5}$ transport for heavy air pollution: study of 5-year observation over central China

Weiyang Hu[1], Tianliang Zhao[1], Yongqing Bai[2], Shaofei Kong[3], Lijuan Shen[1], Jie Xiong[2], Yue Zhou[2], Yao Gu[1], Junnan Shi[4], Huang Zheng[3], and Xiaoyun Sun[1]

[1]Climate and Weather Disasters Collaborative Innovation Center, Key Laboratory for Aerosol-Cloud-Precipitation of China Meteorological Administration, PREMIC, Nanjing University of Information Science &Technology, Nanjing, 210044, China.

[2]Institute of Heavy Rain, China Meteorological Administration, Wuhan, 430205, China.

[3]Department of Atmospheric Sciences, School of Environmental Studies, China University of Geosciences (Wuhan), Wuhan, 430074, China.

[4]Taishan meteorological station of Shandong province, Taishan, 271000, China

Corresponding author: T. Zhao (tlzhao@nuist.edu.cn) and Y. Bai (2007byq@163.com)

Key Points:

- Regional $PM_{2.5}$ transport presents an increasing trend over the past 5 years, dominating heavy pollution events in central China.
- Three regional transport pathways are identified to central China in the northerly, northeasterly, and easterly directions respectively.
- Synoptic circulation modulates regional transport in air quality change with the large contribution to $PM_{2.5}$ over central China.

Abstract

The importance of regional air pollutant transport modulated by large-scale synoptic circulation has been poorly understood for air pollution. In the present study of 5-year (2015-2019) observation, we targeted the Twain-Hu Basin (THB), a region of heavy $PM_{2.5}$ pollution over central China to investigate the regulation of synoptic circulation governing regional $PM_{2.5}$ transport for heavy air pollution. It was found that regional transport of $PM_{2.5}$ predominated 65.2% of the heavy pollution events (HPEs) over the THB based on the statistics of observational environment and meteorology. By employing the FLEXPART-WRF model, the regional transport of $PM_{2.5}$ from upwind source areas in central and eastern China (CEC) to receptor region in the THB was identified with three prominent pathways in the northerly, northeasterly, and easterly directions respectively. Based on T-mode principal component analysis in conjunction with the K-means cluster method, it was recognized that three regional $PM_{2.5}$ transport pathways for the HPEs over central China were determined respectively by three patterns of synoptic circulation over CEC with 1) weak high air pressure to the north, 2) strong high air pressure to the northeast, and 3) weak high air pressure to the east, governing the cold air invasions southwards to the THB region in central China with the large contributions of 76.0%, 56.7%, and 53.9% to the THB- $PM_{2.5}$ concentrations in the HPEs, revealing a significant modulation of large-scale synoptic circulation for regional transport of air pollutants in environmental change.

1 Introduction

$PM_{2.5}$ pollution has aroused worldwide attention owing to its adverse effects on human health (Agarwal et al., 2017; Dang and Liao, 2019), atmospheric visibility (Wang et al., 2020), and direct and indirect impacts on weather and climate (Bi et al., 2016; Zhou et al., 2017; Che et al., 2019). In recent years, high $PM_{2.5}$ levels in the ambient atmosphere during heavy air pollution events have occurred across central and eastern China (CEC), even though the Chinese government has enacted stringent and effective measures to mitigate air pollution, such as the national-scale Air Pollution Prevention and Control Action Plan (Clean Air Plan) in 2013 (China State Council, 2013). Comprehensively understanding the underlying mechanism for frequent heavy air pollution events is of vital importance for improving air quality.

Excessive air pollutant emissions are the primary cause of atmospheric pollution (Su et al., 2019., Zhang et al., 2020). After the Clean Air Plan implementation, air pollution in China mitigated remarkably due to the effective reductions of SO_2, CO, NOx, PM_{10} and primary $PM_{2.5}$ (Fan et al., 2020; Gui et al., 2019; K. Zhang et al., 2019; Zhong et al., 2018). In addition to air pollutant emissions, meteorological conditions play critical roles in controlling the evolution of air pollution events (Chen et al., 2018; Shen et al., 2020a; Zhang et al., 2013; Zhang et al., 2015). Generally, air stagnant conditions of meteorology with weak or calm winds, near-surface thermal inversion layer, and steady atmospheric boundary layers, can impede air pollution dissipation, reinforcing air pollutant accumulations (Chen et al., 2017; Guo et al., 2017; Li et al., 2019; Ren et al., 2017; Zhu et al., 2018). Furthermore, driven by strong winds in multi-scale atmospheric circulations, air pollutants transported from air pollutant source regions can result in deteriorating air quality over the downwind receptor regions, which is a complicated issue in atmospheric environment (Hu et al., 2018; Hu et al., 2021; Huang et al., 2020; Yu et al., 2020).

Meteorological conditions are largely connected with large-scale synoptic circulations. Previous studies have indicated the relationship of air pollution with synoptic circulation in different areas by using circulation-based classification methods, which suggests that synoptic patterns are a key driver of air quality variations (Bei et al., 2016, 2020; Comrie & Yarnal, 1992; Demuzere et al., 2009; He et al., 2016, 2017a; Kalkstein & Corrigan, 1986; Li et al., 2019; Lu et al., 2021; Shahgedanova et al., 1998). For instance, six types of synoptic circulation were identified for wintertime air pollution over North China Plain (NCP) from 2013 to 2018, two of which are prone to outward transport of local $PM_{2.5}$ due to the unstable atmospheric stratification, while the other four types, because of the air stagnation conditions, can elevate local air pollution levels (Wang and Zhang, 2020). Atmospheric circulations can affect air pollution in the Yangtze River Delta (YRD) over eastern China with the southward movement of strong cold air, easterly wind removal, and strong precipitation washout respectively (Hou et al., 2020). Three typical patterns of synoptic circulation including the dry low-trough, high-pressure, and wet low-vortex, were associated respectively with heavy, medium, and slight levels of air pollution determining air quality over the Sichuan Basin (SCB) in southwestern China (Ning et al., 2019). The variations in $PM_{2.5}$ over the Pearl River Delta (PRD) were also connected with different synoptic patterns in southern China (Liao et al., 2020; Liu et al., 2020). However, the driving effect of synoptic circulation on regional transport of $PM_{2.5}$ in heavy air pollution has been poorly understood. Furthermore, how regional $PM_{2.5}$ transport pathways regulated by synoptic circulation was also lack of exploration. A comprehensive understanding of these issues could be helpful for improving air quality.

The Twain-Hu Basin (THB) covers the flat lands over Hubei and Hunan provinces in the middle basin of the Yangtze River over central China (Fig. 1). The THB is a region with heavy air pollution featured by high $PM_{2.5}$ levels over central China, especially during the season of East Asian winter monsoon (Shen et al., 2020b; Zhu et al., 2021). Due to the East Asian winter monsoons' prevailing winds, regional transport of $PM_{2.5}$ plays a dominant part in a heavy air pollution period in centra China with transport contribution of 70.5% (Hu et al., 2021). Although the dominant synoptic patterns were classified for heavy pollution of $PM_{2.5}$ in the region of THB over central China from 2013 to 2018 (Yan et al., 2020), few studies have analyzed the modulation of synoptic circulation on regional $PM_{2.5}$ transport for heavy $PM_{2.5}$ pollution in central China, given that the THB is a key receptor region in regional air pollutant transport over CEC because of its special geographical position with a typical East Asian winter monsoon climate (Yu et al., 2020).

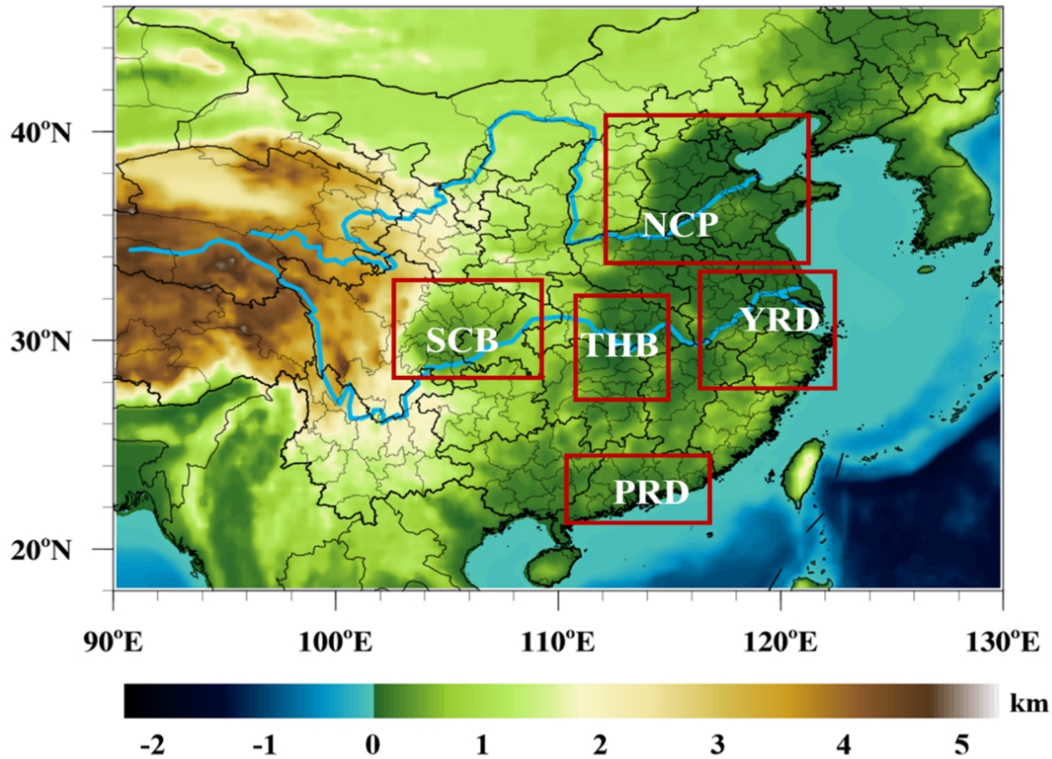

Figure 1. The geographical location of THB, North China Plain (NCP), Yangtze River Delta (YRD), Pearl River Delta (PRD) and Sichuan Basin (SCB) over CEC with the terrain height (km in a.s.l.; shaded contours) from the 2-Minute Gridded Global Relief Data (ETOPO2v2) (http://www.ngdc.noaa.gov/mgg/global/etopo2.html). Two blue lines respectively indicate the Yellow River and Yangtze River in China.

In this study, we characterized the heavy air pollution events (HPEs) affected by regional transport of $PM_{2.5}$ in the THB in central China based on statistics of observation from 2015 to 2019. By using FLEXPART-WRF modeling, we identified three prominent regional $PM_{2.5}$ transport pathways with the contributions to $PM_{2.5}$ concentrations for the HPEs over central China. Besides, we detected the large-scale synoptic systems in regional $PM_{2.5}$ transport through the T-mode principal component analysis (T-PCA) combined with the K-means cluster method and ascertained the regulation of synoptic circulation patterns in three regional $PM_{2.5}$ transport pathways dominating HPEs in central China. We also estimated the regional $PM_{2.5}$ transport's contribution in three major pathways to $PM_{2.5}$ concentrations of the HPEs under different types of synoptic circulation. This study aimed to understand the modulation of large-scale atmospheric circulation for regional transport of air pollutants in environmental change.

2 Data and methods

2.1 $PM_{2.5}$ and meteorological data sources

We used hourly surface $PM_{2.5}$ concentration data observed over CEC over 2015-2019 in this study, which were derived from the National Air Quality Monitoring Network operated by the Ministry of Ecology and Environment of China (http://106.37.208.233:20035/).

The data of sea level pressure (SLP), air temperature and u-, v-, and w-wind components with 0.25 × 0.25° resolution during 2015-2019 were obtained from the ERA5 meteorological reanalysis data of the ECMWF. Moreover, the 5-year observational meteorological data, including near-surface air temperature, relative humidity, SLP, wind speed, wind direction, and precipitation, with 1h temporal resolution, were downloaded from the China meteorological data service center of China Meteorological Administration (http://data.cma.cn/).

2.2 Synoptic circulation classification

T-mode principal component analysis (T-PCA) combined with the K-means cluster was applied to classify the synoptic circulation types for the HPEs in the THB receptor region in regional $PM_{2.5}$ transport over CEC. T-PCA combined with K-means clustering has been widely used in previous studies on environmental change with the reasonable performance in identifying synoptic circulations (Huth, 1996, 2008; He et al., 2017, 2018; Liu et al., 2020; Miao et al., 2017; Zhang et al., 2012).

Three processing steps were used to classify the types of synoptic circulation. First, three-dimensional SLP, were reshaped to two-dimensional dataset (grid × time) and standardized thereafter. Second, the normalized data applying T-PCA with the major components were acquired according to a cumulative variance contribution of 84.0%. Third, through K-means clustering, the main components were selected based on the cluster results. The number of synoptic circulation type classifications relies on the criterion function (Liu and Gao, 2011). Finally, three types of synoptic circulation for regional $PM_{2.5}$ transport for HPEs were ascertained.

The study domain over 20–50° N and 100–130° E in east and north Asian regions includes mainland China and most Mongolian areas. The daily mean SLP data from ERA5 was used to eliminate the biases caused by local small-scale atmospheric circulation, such as land and sea breezes (Hou et al., 2020).

2.3 FLEXPART-WRF model and configuration

The FLEXPART (Stohl et al., 2005; Fast and Easter, 2006), a Lagrangian transport and dispersion model, considering atmospheric physicochemical processes i.e., tracer regional transport, wet and dry depositions, turbulent diffusion (Brioude et al., 2013), was applied in this study to backwards trace the released particle trajectory arriving at the receptor region, further verifying the corresponding air pollutant transport patterns and the spatial distribution of air pollutant source areas that may affect the receptor site.

The WRF model output of meteorology was used to drive the FLEXPART (Skamarock et al., 2008). The NCEP FNL reanalysis data in the horizontal resolution of 1 × 1 ° were applied to provide the initial and boundary conditions for the WRF modeling. The physical process parameterization schemes used in the WRF-simulations included the Lin for microphysics scheme (Lin et al., 1983), RRTM (Mlawer et al., 1997) for long-wave radiation scheme, Goddard (Chou et al., 1999) for short-wave radiation scheme, and YSU scheme (Hong et al., 2006) of the planetary boundary layer (PBL) processes. More details of the WRF model configuration can be found in Table S1.

A 48-h backward trajectory was conducted by FLEXPART-WRF simulation, which released 50000 computational air particles with 0.1 × 0.1° horizontal resolution, centered at a representative THB-site (32.04° N, 112.14° E), namely Xiangyang, for the wintertime HPEs from 2015 to 2019.

2.4 WRF-Modeling validation

The validation of the WRF modeling results with observation of air temperature, wind speed, air pressure, and relative humidity, at the sites Xiangyang, Zhengzhou, Changsha, Hefei, and Nanchang in CEC is shown in Figure S1. The positive correlation coefficients passing the 0.002 significance level and the low normalized standardized deviations were proved to be reasonable in the WRF-modeling, indicating that the meteorology of fine WRF simulation could be used to drive the FLEXPART modeling on the routes of regional air pollutant transport with the contribution to $PM_{2.5}$ concentrations for heavy air pollution in central China.

2.5 Assessment on regional $PM_{2.5}$ transport contribution

Regional $PM_{2.5}$ transport to the receptor region was assessed with the contribution by multiplying the primary $PM_{2.5}$ emission flux by the residential time of air particles from the 48 h backward trajectory simulations of the FLEXPART-WRF, and regional $PM_{2.5}$ transport pathway over CEC could be identified with the spatial distribution of high contribution $rate_{i,j}$ in the following Eq.(1):

$$Contribution\ rate_{i,j} = \frac{E_{i,j} \times r_{i,j}}{\sum_{1,1}^{N,S} E_{i,j} \times r_{i,j}} \tag{1}$$

where i and j stand for the grid location (*i, j*) from the first grid cell (i=*1*, j=*1*) to the last grid cell (j=*N, j*=*S*) over CEC on the 48-h backward trajectory, $r_{i,j}$ means $PM_{2.5}$ residential time from the FLEXPART-WRF simulation, and $E_{i,j}$ manifests the $PM_{2.5}$ emission intensity over the grid at location (*i, j*) from the Multi-resolution Emission Inventory for China (MEIC; http://www.meicmodel.org/).

$$R = \sum_{(N_1,S_1)}^{(N_2,S_2)} rate_{i,j} \tag{2}$$

R means the total contribution of regional transport of $PM_{2.5}$ from the external regions over the first and last grid cells respectively at (N_1, S_1) and (N_2, S_2) over the non-local emission sources to the HPEs in the THB receptor region over central China through the FLEXPART-WRF simulation (Yu et al., 2020 ; Chen et al.,2017).

3 Results and Discussion

3.1 Regional transport of $PM_{2.5}$ dominating heavy air pollution

Firstly, 46 days of regional HPEs over the THB from 2015 to 2019 were detected with the daily averaged surface $PM_{2.5}$ concentrations greater or equal than 150 μg m^{-3} observed at three or more sites, which all happened in the East Asian winter monsoon season from November to following March (Table S2), reflecting a close linkage of the seasonal shift of East Asian monsoons with regional change of atmospheric environment. Then, based on the climatology of cold air invasion with southward advance of high air pressure system from northern China triggered by East Asian winter monsoonal winds (Ding, 1993; Hou et al., 2020; Wang et al., 2020), we established the criterion for wintertime regional transport of air pollutants to the THB with the sea level pressure gradient (> 3.0 hPa) between 33° N and 26° N averaged over 112° E-

114° E and the regional average meridional component (< -1.0 m s^{-1}) of near-surface wind. According to this criterion, 30 days of HPEs in central China connecting with regional transport of $PM_{2.5}$ were selected out among the 46 days of regional HPEs based on the statistics of observed HPEs over 2015-2019. Therefore, it was estimated with the ratio of 30/46 days of regional HPEs that 65.2% of the HPEs in the THB during the recent 5 years were influenced by the regional $PM_{2.5}$ transport with strong near-surface northerly (meridional) winds.

Generally, air pollution is formed by local accumulation and regional air pollutant transport (Chen et al., 2017; Yu et al., 2020; Zhu et al., 2018). Figure 2 displays the proportion (%) of the HPEs affected by regional $PM_{2.5}$ transport during total HPEs for assessing the impacts of regional transport and local accumulation on the change of HPEs over the THB from 2015 to 2019. The HPEs influenced with regional $PM_{2.5}$ transport were accounted for 64.3%, 70.0%, 37.5%, 75.0%, and 100.0% over 2015-2019 (Fig. 2), presenting an increasing trend in the dominant contribution of regional transport of $PM_{2.5}$ to the HPEs over the recent years, which is distinguished from the local accumulation of air pollutants under the stagnant air conditions causing the HPEs in most regions over CEC (Cai et al., 2017; Shu et al., 2021; Zhang et al., 2018; Zhong et al., 2019).

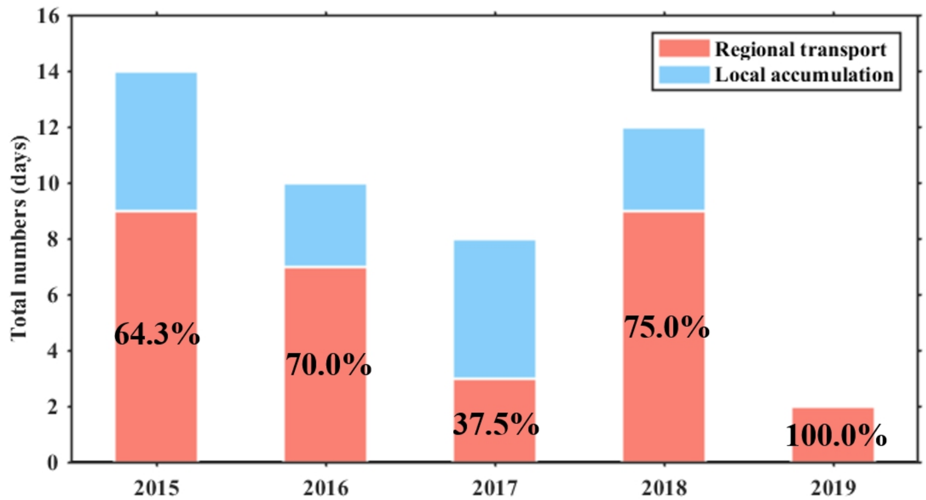

Figure 2. Annual occurrence days of regional transport (red column) and local accumulation (blue column) in the regional HPEs over the THB in central China from 2015 to 2019. The percentages mean the proportion of HPEs dominated with regional $PM_{2.5}$ transport.

3.2 Identifying pathways and contribution of regional transport

In section 3.1, we found the dominance of regional transport of $PM_{2.5}$ during the HPEs based on the statistics of observation over the THB from 2015 to 2019. In this section, the pathways of regional $PM_{2.5}$ transport from upwind areas to the THB in central China were recognized with quantifying the corresponding contribution to the HPEs through the residence time of air particle tracer simulated by the FLEAXPART-WRF and the $PM_{2.5}$ emission flux over the air pollutant sources in CEC with Eqs. (1) and (2).

The major pathways of regional transport to the downwind receptor region could be identified with high contribution rates of regional transport to $PM_{2.5}$ pollution events (Yu et al., 2020). Figure 3 displays the average distribution of regional transport pathways with high $PM_{2.5}$ contribution rates of sources to the THB in central China for 30 days of regional HPEs from 2015 to 2019. It was recognized from Figure 3 that $PM_{2.5}$ from regional transport to the THB-region during the HPEs is climatologically centered on three typical transport routes in the northerly, northeasterly, and easterly transport directions, respectively. Furthermore, the dominant $PM_{2.5}$ contribution of regional transport emitted from non-local regions over CEC to $PM_{2.5}$ concentrations for HPEs in the THB in central China from 2015 to 2019 was averaged as 60.2% (Table S3), revealing a determining part of $PM_{2.5}$ transported from the upwind source areas in worsening air environment over central China from a long-term perspective.

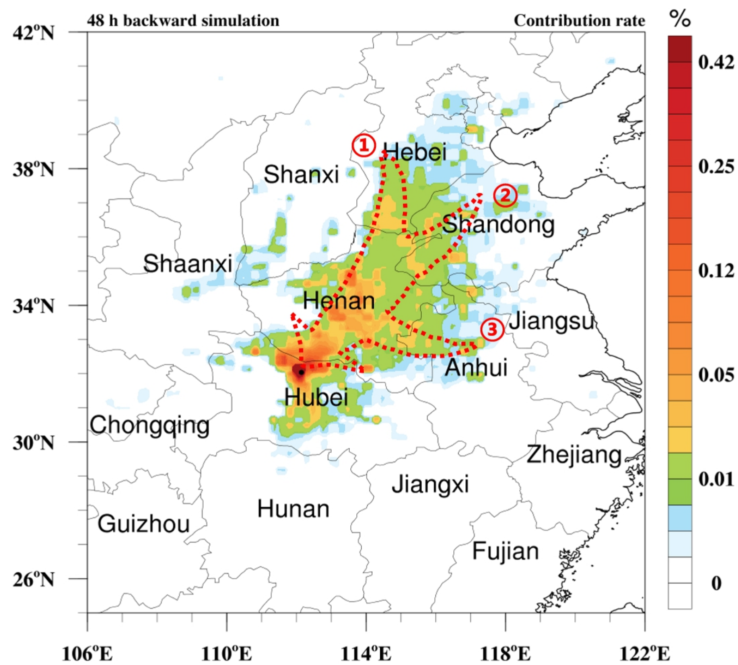

Figure 3. Distribution of averaged contribution rates (color contours) to surface $PM_{2.5}$ during 30 heavy pollution days in the THB from 2015 to 2019 with three dominant regional $PM_{2.5}$ transport pathways (red dashed arrows) in the ① northerly, ② northeasterly and ③ easterly directions over CEC.

Since the synoptic circulation exert a strong influence on $PM_{2.5}$ concentrations over CEC (He et al., 2017a; He et al., 2017b; He et al., 2018; Zong et al., 2021), the regulation of synoptic circulation on building the three routes of regional transport from the upwind sources over CEC to central China for the downwind regional HPEs (Fig. 3), require an in-depth exploration to improve the understanding in air quality change.

3.3 Synoptic circulation in regional $PM_{2.5}$ transport to HPEs

The T-PCA combined with K-means cluster classification was applied to the HPEs with regional $PM_{2.5}$ transport, and three dominant synoptic circulation types were identified (Table S4). Figure 4 shows the anomalous patterns of sea level pressure (SLP) in three dominant synoptic circulation types. As the typical feature of East Asian winter monsoon, the cold air masses sweep across CEC with the southward advance of high-pressure system, whose shifting location and intensity alter the weather process and meteorological elements (Ding, 1993; Ding et al., 2017). According to the location and intensity of high-pressure systems over CEC with cold air southward invasion driving regional $PM_{2.5}$ transport to the THB for the HPEs, three dominant synoptic patterns were described as strong high pressure to the northeast (CT1), weak high pressure to the east (CT2), and weak high pressure to the north (CT3).

The synoptic circulation type CT1 was the most frequent, accounting for 46.7% of the total synoptic circulation. For CT1, a strong high-pressure system originating in the Siberian region extended from Mongolia to China (Fig. S3). In this pattern, northeasterly wind anomalies prevailed in northern China (NC) and changed to northerly winds into the THB over central China (Fig. 4a) accompanied by the negative anomalies of air temperature in the vertical layers for the strong cold air invasion (Fig. S2a), with wind speed of 2.6 m s^{-1} (Table S5), transporting air pollutants from NC to the THB. The CT2 occurrence frequency was 40.0%. In CT2, a weak surface air pressure with anticyclone was situated northeasterly to the THB over China (Fig. 4b), which was nearly controlled by the warm air mass anomalies (Fig. S2b) with the 2-m air temperature increasing up to 7.4 ℃ (Table S5). In this pattern, the prevailing easterly winds cover east China with the average wind speed of 2.7 m s^{-1} (Table S5) in the THB, which is conducive to bringing air pollutants from eastern China, mainly the YRD to the THB. The CT3, from Mongolia region to northern China (Fig. S4) was the relatively week high-pressure system differing from the CT1 (Figs. 4c and 5c) with 3.1 m s^{-1} averaged wind speed over the THB in the north direction (Table S5), strengthening $PM_{2.5}$ transport from non-local source areas to the THB for the HPEs.

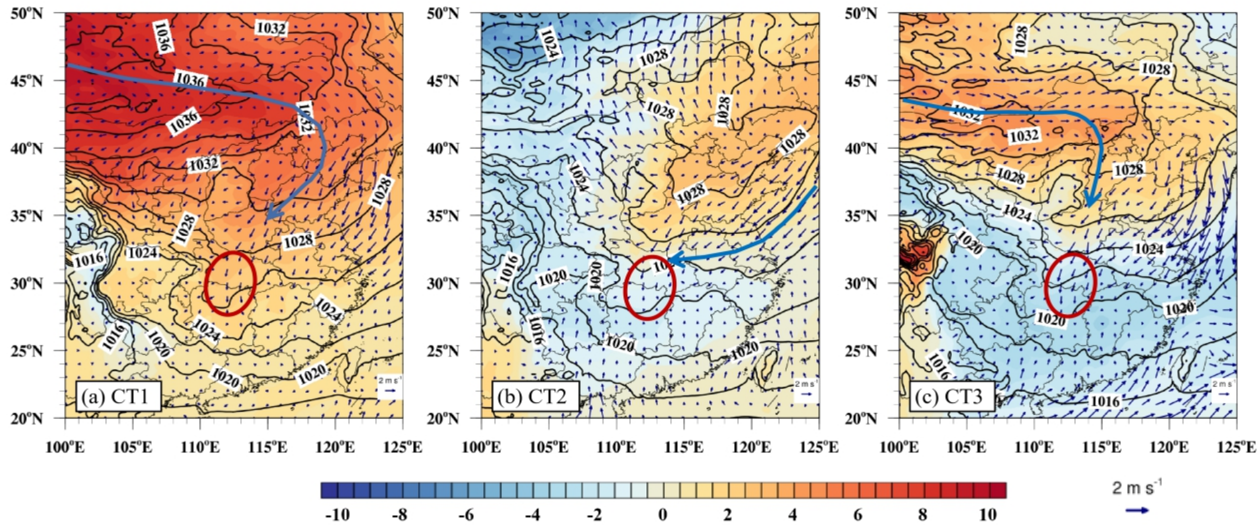

Figure 4. The average daily SLP (black lines; hPa) and 10-m wind vector anomalies (m s^{-1}) in the three synoptic circulation patterns (a) CT1, (b) CT2 and (c) CT3 for the wintertime HPEs dominated by regional $PM_{2.5}$ transport from 2015 to 2019 with the anomalies of daily SLP (color contours; hPa) over CEC. The wind (SLP) anomalies were relatively with the 5-year wintertime mean of winds (SLP). Blue thick lines with arrows mean the dominant southward routes of cold air invasions, and red circles roughly outline the THB areas in central China.

3.4 Modulation of synoptic circulation on regional transport of $PM_{2.5}$

Aiming to explore the modulation of synoptic circulation on $PM_{2.5}$ from regional transport to the HPEs over central China, we investigated the synoptic circulation evolution affected $PM_{2.5}$ transported from upwind areas over CEC to the THB. Figure 5 exhibits the evolution of three synoptic circulations and the changes in $PM_{2.5}$ concentrations during the regional transport of $PM_{2.5}$ over CEC. It shows that synoptic circulation evolution with different location and intensity of advancing high air pressure in anticyclone could build three routes of regional $PM_{2.5}$ transport from the upwind source regions to downwind regional HPEs in CEC (Fig. 5).

In CT1, the positive SLP anomalies existed over the northern CEC. In the beginning of the THB's heavy air pollution, weak winds engendered the air pollutant accumulations over the northern CEC with high surface $PM_{2.5}$ levels over the NCP (Fig. 5a). At the developing stage (Fig. 5b), as the relatively strong cold air mass from Mongolia moved southwards, weak winds gradually turned into strong northeasterly wind fields over the northern CEC. With the southward advance of cold air mass, high $PM_{2.5}$ concentrations from the upstream areas over

CEC were transported to the downwind regions, mainly the THB, and $PM_{2.5}$ concentrations over the NCP significantly decreased (Fig. 5c).

With CT2, the weak high-pressure anomalies moved southeastwards over CEC with prevailing northerly and northwesterly winds, leading to $PM_{2.5}$ transport to the downstream areas (Figs. 6d-6e). On the day of heavy air pollution in the THB, the high pressure was shifted in the southeast direction and finally covered northeastern China with obvious northeasterly winds over the YRD. $PM_{2.5}$, therefore, was transported finally to the THB in the easterly winds over central China (Fig. 5f).

During CT3, there was an apparent low-pressure system occupied over CEC 1-2 days before the HPEs over the THB (Figs. 6g and 6h). The air pollution levels over the NCP in the northern CEC were the most serious among three synoptic circulation types (Figs. 6h and 6g). A strong cold air mass moved southward from Mongolia to NCP, driving $PM_{2.5}$ from the NCP to the downstream areas (Fig. 5h), $PM_{2.5}$ parcels over the NCP were transported to the THB by the prevailing northerly winds in the CT3 (Fig. 5i).

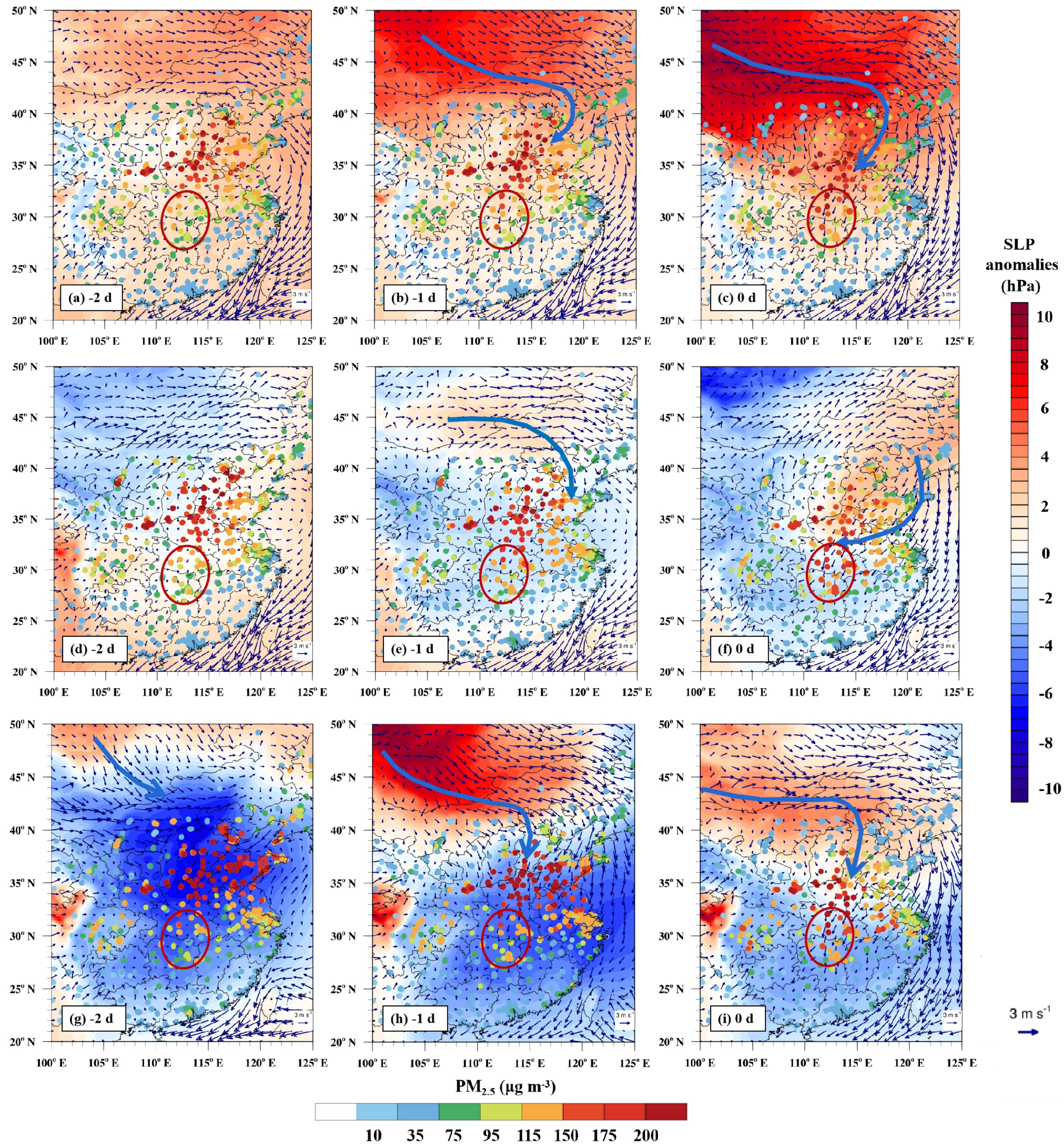

Figure 5. Spatial distribution of 10-m wind vectors (m s^{-1}), SLP anomalies (hPa; color contours) and $PM_{2.5}$ concentrations (μg m^{-3}; color dots) at (a, d, g) 2 days and (b, e, h) 1 day before the HPEs as well as (c, f, i) at the day of HPEs dominated with regional $PM_{2.5}$ transport over CEC. Blue thick lines with arrows mean the dominant routes of cold air southward invasions, and a-c, d-f, and g-i represent the evolution of synoptic circulation types CT1, CT2, and CT3, respectively.

Overall, with the southward cold air movement during the season of East Asian winter monsoon, $PM_{2.5}$-rich air mass from the NCP and YRD over CEC was along three main regional transport routes to the THB for the regional HPEs with northerly northeasterly and easterly directions, respectively, basically governed by three patterns of synoptic circulation over CEC with: 1) weak high pressure to the north (CT3), 2) strong high pressure to the northeast (CT1), and 3) weak high pressure to the east (CT2) to the THB over central China, differing from the unfavorable meteorological conditions with weak winds and thermal inversion layer for the HPEs observed in the other air polluted areas of CEC (Ding et al., 2017; Huang et al., 2018). This study revealed a significant modulation of synoptic circulation for regional transport of air pollutants in air quality change.

3.5 Contributions of regional $PM_{2.5}$ transport to HPEs under three types of synoptic circulation

Given that three synoptic circulation types CT1, CT2, and CT3 could govern regional $PM_{2.5}$ transport along the northeasterly, easterly and northerly pathways over CEC, we further evaluated the contribution of three regional $PM_{2.5}$ transport under three types of synoptic circulation to $PM_{2.5}$ concentrations for the wintertime HPEs occurring over the THB over central China with the FLEXPART-WRF model.

By calculating the contribution rates with the Eq. (1), we evaluated the contribution rates of regional $PM_{2.5}$ transport from non-local regions to $PM_{2.5}$ concentrations over central China under three synoptic circulation types CT1, CT2 and CT3. Figure 6 displayed the three corresponding spatial distributions of contribution to $PM_{2.5}$ concentrations for HPEs in the THB. As displayed in Figure 6a, regional transport of $PM_{2.5}$ was obviously centered on the northeasterly route from CEC to the THB over central China during CT1. As for CT2, the easterly pathway of regional transport was clearly recognized with the high $PM_{2.5}$ contribution rates from the YRD to the THB over the CEC (Fig. 6b). Along the northerly regional transport pathway of $PM_{2.5}$, high $PM_{2.5}$ sourced from the NCP could enhance air pollution levels for HPEs over central China during CT3 (Fig. 6c).

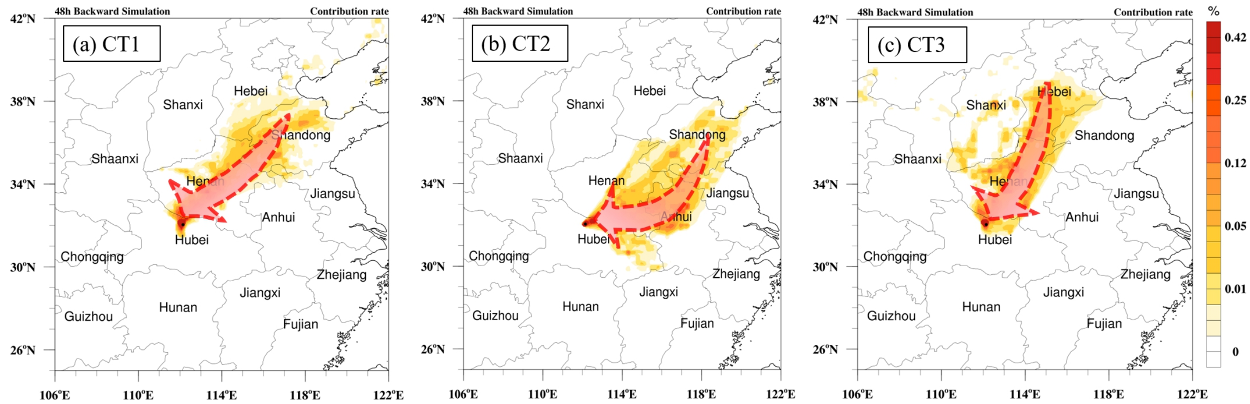

Figure 6. Distribution of contribution rates (color contours) to surface $PM_{2.5}$ over the THB in three major pathways (red dash arrows) of regional $PM_{2.5}$ transport over CEC under three synoptic circulation types (a) CT1, (b) CT2, and (c) CT3 during the wintertime HPEs in the THB from 2015 to 2019 simulated by the FLEXPART-WRF model.

Besides, the contributions of regional transport from non-local regions over CEC to $PM_{2.5}$ pollution over the THB in central China under CT1, CT2, and CT3 were estimated by using Eq. (2). As shown in Table 1, regional $PM_{2.5}$ transport contributed 56.7%, 53.9%, and 76.0% to surface $PM_{2.5}$ in the HPEs over central China during CT1, CT2, and CT3 respectively, indicating the dominance of regional $PM_{2.5}$ transport modulated by large-scale synoptic circulation in enhancing $PM_{2.5}$ levels for HPEs over central China, which could have an implication for regional joint control on air pollution over CEC (Bai et al., 2021; Shen et al., 2020a).

Table 1. Averaged contribution rates of regional $PM_{2.5}$ transport and local emissions over the THB in central China under three synoptic circulation types CT1, CT2 and CT3.

Contribution rates	CT1	CT2	CT3
Regional transport	56.7%	53.9%	76.0%
Local emissions	43.3%	46.1%	24.0%

4 Conclusions

In the present study, we characterized heavy air pollution driven by regional transport of $PM_{2.5}$ occurring in central China, explored the large-scale synoptic circulation influencing regional $PM_{2.5}$ transport with corresponding contributions to $PM_{2.5}$ concentrations during the HPEs from 2015 to 2019 through the analyses of meteorological and environmental observations, T-mode principal component method (T-PCA) combined with the K-means cluster, and FLEXPART–WRF model simulations.

Approximately 65.2% of the HPEs in the THB over central China were triggered by regional transport of $PM_{2.5}$ over CEC. Based on simulations of the FLEXPART–WRF model, regional transport of $PM_{2.5}$ was centered along three routes in the northerly, northeasterly and easterly directions respectively. In addition, regional $PM_{2.5}$ transport quantitatively contributed 60.2% to $PM_{2.5}$ concentrations to HPEs in the THB over central China from 2015 to 2019, presenting regional $PM_{2.5}$ transport in aggravating air pollution levels over central China from a long-term perspective.

The southward invasion of cold air was the vital driving factor for transporting $PM_{2.5}$ from upwind regions over the CEC to the HPEs in central China, which is closely related to the evolution of synoptic circulation. By using T-mode principal component analysis (T-PCA) combined with the K-means cluster method, we identified three synoptic circulation types: 1) strong high pressure to the northeast, 2) weak high pressure to the east, and 3) weak high pressure to the north that builded three regional $PM_{2.5}$ transport routes to central China in the northeasterly, easterly, and northerly directions with the $PM_{2.5}$ contributions of 56.7%, 53.9%, and 76.0% to the HPEs, respectively, revealing an important effect of large-scale atmospheric circulations on regional transport of $PM_{2.5}$ causing HPEs over central China.

Possible uncertainties could exist in this study without consideration the regional transport of gaseous precursors of $PM_{2.5}$ during HPEs and with the classification of synoptic patterns with sea level pressure. Long-term observation data and comprehensive models of environment and meteorology could improve our understanding of regional air pollutant transport regulated by large-scale atmospheric circulation on atmospheric environment change.

Competing interests: The authors declare that they have no conflicts of interest.

Acknowledgement: This study was jointly funded by the National Natural Science Foundation of China (42075186; 41830965; 91744209).

Data availability statement: The meteorology inputs for WRF model and T-PCA with K-means cluster are available from NCAR (https://rda.ucar.edu/datasets/ds083.2/index.html#sfol-wl-/data/ds083.2?g=2) and ECMWF (https://cds.climate.copernicus.eu/cdsapp#!/dataset/reanalysis-era5-single-levels?tab=form) respectively. The hourly meteorological data is sourced from http://data.cma.cn/. The hourly $PM_{2.5}$ data are acquired from National Air Quality Monitoring Network operated by the Ministry of Ecology and Environment of China (http://106.37.208.233:20035/). The data of Multi-resolution Emission Inventory for China was from http://www.meicmodel.org/.

References

Agarwal, N. K., Sharma, P., & Agarwal, S. K. (2017), Particulate matter air pollution and cardiovascular disease. *Medicine Science*, *21*, 270-279. doi:10.1161/cir.0b013e3181dbece1

Bai, Y., Zhao, T., Zhou, Y., Kong, S., Hu, W., Xiong, J., Liu, L., Zheng, H., & Meng, K. (2021), Aggravation effect of regional transport on wintertime $PM_{2.5}$ over the middle reaches of the Yangtze River under China's air pollutant emission reduction process. *Atmospheric Pollution Research*, *12*(7), 101111. doi: 10.1016/j.apr.2021.101111

Bei, N., Li, G., Huang, R., Cao, J., Meng, N., Feng, T., Liu, S., Zhang, T., Zhang, Q., & Molina, L. (2016), Typical synoptic situations and their impacts on the wintertime air pollution in the Guanzhong basin, China. *Atmospheric Chemistry and Physics*, *16*, 7373–7387. doi:10.5194/acp-2015-710

Bei, N., Li, X., Tie, X, Zhao, L., Wu, J., Li, X., Liu L., Shen Z., & Li G. (2020), Impact of synoptic patterns and meteorological elements on the wintertime haze in the Beijing-Tianjin-Hebei region, China from 2013 to 2017. *Science of the Total Environment*, *704*, 12. doi: 10.1016/j.scitotenv.2019.135210

Bi, J., Huang, J., Holben, B., & Zhang, G. (2016), Comparison of key absorption and optical properties between pure and transported anthropogenic dust over East and Central Asia. *Atmospheric Chemistry and Physics*, *16*, 15501–15516. doi:10.5194/acp-16-15501-2016

Brioude, J., Arnold, D., Stohl, A., Cassiani, M., Morton, D., Seibert, P., Angevine, W., Evan, S., Dingwell, A., Fast, J. D., Easter, R. C., Pisso, I., Burkhart, J., & Wotawa, G. (2013), The Lagrangian particle dispersion model FLEXPART-WRF version 3.1. *Geoscientific Model Development*, *6*, 1889–1904. doi:10.5194/gmd-6-1889-2013

Cai, W., Li, K., Liao, H., Wang, H., & Wu, L. (2017), Weather conditions conducive to Beijing severe haze more frequent under climate change. *Nature Climate Change*, *7*, 257–262. doi:10.1038/nclimate3249

Che, H., Xia, X., Zhao, H., Dubovik, O., Holben, B. N., Goloub, P., Cuevas-Agulló, E., Estelles, V., Wang, Y., Zhu, J., Qi, B., Gong, W., Yang, H., Zhang, R., Yang, L., Chen, J., Wang, H., Zheng, Y., Gui, K., Zhang, X. C., & Zhang X. Y. (2019), Spatial distribution of aerosol microphysical and optical properties and direct radiative effect from the China Aerosol Remote Sensing Network. *Atmospheric Chemistry and Physics*, *19*, 11843–11864. doi:10.5194/acp-2019-405

Chen, S., Zhou, G., & Zhu, B. (2017), A method for fast quantification of air pollutant sources. *Acta Scientiae Circumstantiae* (in Chinese), 37, 2474–2481. doi:10.13671/j.hjkxxb.2017.0045

Chen, Z., Cai, J., Gao, B., Xu, B., Dai, S., He, B., & Xie, X. (2017). Detecting the causality influence of individual meteorological factors on local PM$_{2.5}$ concentrations in the Jing-Jin-Ji region. *Scientific Report*, *7*, 40735. doi:10.1038/srep40735

Chen, Z., Xie, X., Cai, J., Chen, D., Gao, B., He, B., Cheng, N., & Xu, B. (2018), Understanding meteorological influences on PM$_{2.5}$ concentrations across China: a temporal and spatial perspective. *Atmospheric Chemistry and Physics*, *18*, 5343–5358. doi:10.5194/acp-18-5343-2018

Chou, M., Suarez, M., Ho, C., Yan, M., & Lee, K. (1998). Parameterizations for Cloud Overlapping and Shortwave Single-Scattering Properties for Use in General Circulation and Cloud Ensemble Models. *Journal of Climate*, *11*, 202–214. doi: 10.1175/1520-0442(1998)011<0202:PFCOAS>2.0.CO;2.

China State Council: Action Plan on Prevention and Control of Air Pollution, China State Council, Beijing, China, available at:http://www.gov.cn/zwgk/2013-09/12/content_2486773.htm (last access: 06 May 2021), 2013.

Comrie, A. C., & Yarnal, B. (1992), Relationships between synoptic-scale atmospheric circulation and ozone concentrations in metropolitan Pittsburgh, Pennsylvania. *Atmospheric Environment*, *26*, 301–312. doi:10.1016/0957-1272(92)90006-E

Dang, R., & Liao, H. (2019), Severe winter haze days in the Beijing–Tianjin–Hebei region from 1985 to 2017 and the roles of anthropogenic emissions and meteorology. *Atmospheric Chemistry and Physics*, *19*(16), 10, 801–10,816. doi:10.5194/acp-19-10801-2019

Demuzere, M., Trigo, R.M., Vila-Guerau de Arellano, J., & van Lipzig, N.P.M. (2009), The impact of weather and atmospheric circulation on O$_3$ and PM$_{10}$ levels at a rural mid-latitude site. *Atmospheric Chemistry and Physics*, *9*, 2695–2714. doi: 10.5194/acp-9-2695-2009

Ding, Y. (1993), Monsoons over china, *Springer Science & Business Media*.

Ding, Y., Wu, P., Liu, Y., & Song, Y. (2017), Environmental and Dynamic Conditions for the Occurrence of Persistent Haze Events in North China. *Engineering*, *3*, 266–271, doi:10.1016/j.eng.2017.01.009

Fan, H., Zhao, C., & Yang, Y. (2020), A comprehensive analysis of the spatio-temporal variation of urban air pollution in China during 2014-2018. *Atmospheric Environment*, *220*, 117066. doi:10.1016/j.atmosenv.2019.117066.

Fast, J. D. & Easter, R. C. (2006), A Lagrangian particle dispersion model compatible with WRF, *7th WRF Users Workshop, NCAR*, 19–22.

Gui, K., Che, H., Wang, Y., Wang, H., Zhang, L., Zhao, H., Zheng, Y., Sun, T., & Zhang, X. (2019), Satellite-derived $PM_{2.5}$ concentration trends over Eastern China from 1998 to 2016: Relationships to emissions and meteorological parameters. *Environmental Pollution*, *247*, 1125−1133. doi:10.1016/j.envpol.2019.01.056

Guo, H., Wang, Y., & Zhang, H. (2017), Characterization of criteria air pollutants in Beijing during 2014−2015. *Environmental Research*, *154*, 334–344. doi:10.1016/j.envres.2017.01.029

He, J., Wu, L., Mao, H., Liu, H., Jing, B., Yu, Y., Ren, P., Feng, C., & Liu, X. (2016), Development of a vehicle emission inventory with high temporal–spatial resolution based on NRT traffic data and its impact on air pollution in Beijing-Part 2: impact of vehicle emission on urban air quality. *Atmospheric Chemistry and Physics*, *16*, 3171–3184. doi:10.5194/acp-16-3171-2016

He, J., Gong, S., Yu, Y., Yu, L., Wu, L., Mao, H., Song, C., Zhao, S., Liu, H., Li, X., & Li, R. (2017a), Air pollution characteristics and their relationship to meteorological conditions during 2014-2015 in Chinese major cities. *Environmental Pollution*, *223*, 484–496. doi:10.1016/j.envpol.2017.01.050

He, J., Gong, S., Liu, H., An, X., Yu, Y., Zhao, S., Wu, L., Song, C., Zhou, C., Wang, J., Yin,C., & Yu, L. (2017b), Influences of meteorological conditions on interannual variations of particulate matter pollution during winter in the Beijing–Tianjin–Hebei area. *Journal of Meteorological Research*, *31*(6), 1062–1069. doi:10.1007/s13351-017-7039-9

He, J., Gong, S., Zhou, C., Lu, S., Wu, L., Chen, Y., Ye, Y., Zhao, S., Yu L., & Yin, C. (2018), Analyses of winter circulation types and their impacts on haze pollution in Beijing. *Atmospheric Environment*, *192*, 94–103. doi:10.1016/j.atmosenv.2018.08.060

Hu, J., Li, Y., Zhao, T., Liu J., Hu X., Liu, D., Jiang, Y., Xu, J., & Chang L. (2018), An important mechanism of regional O_3 transport for summer smog over the Yangtze River Delta in eastern China. *Atmospheric Chemistry and Physics*, *18*(22), 16239−16251. doi:10.5194/acp-18-16239-2018

Hu, W., Zhao, T., Bai, Y., Kong, S., Xiong, J., Sun, X., Yang, Q., Gu, Y., & Lu, H. (2021), Importance of regional $PM_{2.5}$ transport and precipitation washout in heavy air pollution in the Twain-Hu Basin over Central China: Observational analysis and WRF-Chem simulation. *Science of the Total Environment*, 143710. doi:10.1016/j.scitotenv.2020.143710

Hu, W., Zhao, T., Bai, Y., Shen, L., Sun, X., & Gu, Y. (2020), Contribution of Regional $PM_{2.5}$ Transport to Air Pollution Enhanced by Sub-Basin Topography: A Modeling Case over Central China. *Atmosphere*, *11*(11). doi: 10.3390/atmos11111258, 2020.

Huang, Q., Cai, X., Wang, J., Song, Y., & Zhu, T. (2018), Climatological study of the Boundary-layer air

Stagnation Index for China and its relationship with air pollution. *Atmospheric Chemistry and Physics*, *18*, 7573–7593. doi:10.5194/acp-18-7573-2018

Huang, X., Ding, A., Wang, Z., Ding, K., Gao, J., Chai, F., & Fu, C. (2020), Amplified transboundary transport of haze by aerosol–boundary layer interaction in China. *Nature Geoscience*, *13*, 428-434. doi:10.1038/s41561-020-0583-4

Huth, R. (1996), An intercomparison of computer-assisted circulations classification methods. *International Journal of Climatology*, *16*, 893–922. doi:10.1002/(SICI)1097-0088(199608)16:8<893::AID-JOC51>3.0.CO;2-Q

Huth, R., Beck, C., Philipp, A., Demuzere, M., Ustrnul, Z., Cahynová, M., Kyselý, J., & Tveito OE. (2008), Classifications of atmospheric circulation patterns: Recent advances and applications. *Annals, New York Academy of Sciences*, *1146*, 105–152. doi: 10.1196/annals.1446.019

Hong, S., Noh, Y., & Dudhia, J. (2006), A New Vertical Diffusion Package with an Explicit Treatment of Entrainment Processes. *Monthly Weather Review*, *134*, 2318–2341. doi:10.1175/MWR3199.1

Hou, X., Zhu, B., Kumar, K. R., de Leeuw,G., Lu,W., Huang, Q., & Zhu, X. (2020), Establishment of conceptual schemas of surface synoptic meteorological situations affecting fine particulate pollution across eastern China in the winter. *Journal of Geophysical Research-Atmospheres*, *125*, e2020JD033153. doi:10.1029/2020JD033153

Kalkstein, L. S., & Corrigan, P. (1986) A synoptic climatological approach for geographical analysis: Assessment of sulfur dioxide concentrations. *Annals of the Association of American Geographers*, *76*, 381–395. doi:10.1111/j.1467-8306.1986.tb00126.x

Li, J., Liao, H., Hu, J., & Li, N. (2019), Severe particulate pollution days in China during 2013–2018 and the associated typical weather patterns in Beijing-Tianjin-Hebei and the Yangtze River Delta regions. *Environmental Pollution*, *248*, 74–81. doi:10.1016/j.envpol.2019.01.124

Li, X., Hu, X.M., Ma, Y., Wang, Y., Li, L., & Zhao, Z. (2019), Impact of planetary boundary layer structure on the formation and evolution of air-pollution episodes in Shenyang, Northeast China. *Atmospheric Environment*, *214*, 116850. doi:10.1016/j.atmosenv.2019.116850

Lin, Y., Farley, R., & Orville, H. (1983), Bulk Parameterization of the Snow Field in a Cloud Model. *Journal of Applied Meteorology and Climatology*, *22*(6), 1065–1092. doi:10.1175/1520-0450(1983)022<1065:BPOTSF>2.0.CO;2

Lu, H., Ma, C., Zhao, T., Meng, K., Zheng, X., Li, J., Lu, P., & Liu, H. (2021), Analysis of synoptic pattern on

$PM_{2.5}$ heavy pollution over the Beijing-Tianjin-Hebei region in winter based on PCT. *Acta Scientiae Circumstantiae* (in Chinese), *41*(3), 898-904. doi:10.13671/j.hjkxxb.2020.0532

Liao, Z., Xie, J., Fang, X., Wang, Y., Zhang, Y., Xu, X., & Fan, S. (2020), Modulation of synoptic circulation to dry season $PM_{2.5}$ pollution over the Pearl River Delta region: An investigation based on self-organizing maps. *Atmospheric Environment*, *230*, 117482. doi:10.1016/j.atmosenv.2020.117482

Liu, Y., He, J., Lai, X., Zhang, C., & Che, H. (2020), Influence of atmospheric circulation on aerosol and its optical characteristics in the pearl river delta region. *Atmosphere*, *11*(3), 288. doi:10.3390/atmos11030288

Mlawer, E., Taubman, S., Brown, P., Iacono, M., & Clough, S. (1997), Radiative transfer for inhomogeneous atmospheres: RRTM, a validated correlated-k model for the longwave. *Journal of Geophysical Research- Atmospheres*, *102*(D14), 16663–16682. doi:10.1029/97jd00237

Miao, Y., Guo, J., Liu, S., Liu, H., Li, Z., Zhang, W., & Zhai, P. (2017), Classification of summertime synoptic patterns in Beijing and their associations with boundary layer structure affecting aerosol pollution. *Atmospheric Chemistry and Physics*, *17*, 3097–3110. doi:10.5194/acp-17-3097-2017

Ning, G., Yim, S.H.L., Wang, S., Duan, B., Nie, C., Yang, X., Wang, J., & Shang, K. (2019), Synergistic effects of synoptic weather patterns and topography on air quality: a case of the Sichuan Basin of China. *Climate Dynamics*, *53*, 6729–6744. doi:10.1007/s00382-019-04954-3

Ren, Y., Zheng, S., Wei, W., Wu, B., Zhang, H., Cai, X., & Song, Y. (2018), Characteristics of turbulent transfer during episodes of heavy haze pollution in Beijing in Winter 2016/17. *Journal of Meteorological Research*, *32*(1), 69–80. doi: 10.1007/s13351-018-7072-3

Shahgedanova, M., Burt, T., & Davies, T. (1998), Synoptic climatology of air pollution in Moscow. *Theoretical and Applied Climatology*, *61*, 85–102. doi:10.1007/s007040050054

Shen, L., Zhao, T., Wang, H., Liu, J., Bai, Y., Kong, S., Zheng, H., Zhu, Y., & Shu, Z. (2020a), Importance of meteorology in air pollution events during the city lockdown for COVID-19 in Hubei Province, Central China. *Science of the Total Environment*, *754*, 142227. doi:10.1016/j.scitotenv.2020.142227

Shen, L., Wang, H., Zhao, T., Liu, J., Bai, Y., Kong, S., & Shu, Z. (2020b), Characterizing regional aerosol pollution in Central China based on 19 years of MODIS data: Spatiotemporal variation and aerosol type discrimination. *Environmental Pollution*, *263*, 114556. doi:10.1016/j.envpol.2020.114556

Shu, Z., Liu Y., Zhao, T., Xia, J., Wang, C., Cao, L., Wang, H., Zhang, L., Zheng, Y., Shen, L., Luo, L., & Li, Y. (2021), Elevated 3D structures of $PM_{2.5}$ and impact of complex terrain-forcing circulations on heavy haze pollution over Sichuan Basin, China. *Atmospheric Chemistry and Physics*, *21*(11), 9253-9268. doi: 10.5194/acp-21-9253-2021

Skamarock, W. C., Klemp, J. B., Dudhia, J., Gill, D. O., Barker, D. M., Duda, M., Huang, X.-Y., Wang, W., & Powers, J. G. (2008), A Description of the Advanced Research WRF Version 3, NCAR Technical Note, Boulder, CO, USA. doi:10.13140/RG.2.1.2310.6645

Stohl, A., Forster, C., Frank, A., Seibert, P., & Wotawa, G. (2005), Technical note: The Lagrangian particle dispersion model FLEXPART version 6.2. *Atmospheric Chemistry and Physics*, *5*, 2461 – 2474, doi:10.5194/acp-5-2461-2005

Su, W., Liu, C., Hu, Q., Zhao, S., Sun, Y., Wang, W., Zhu, Y., Liu, J., & Kim, J. (2019), Primary and secondary sources of ambient formaldehyde in the Yangtze River Delta based on ozone mapping and profiler suite (OMPS) observations. *Atmospheric Chemistry and Physics*, *19*, 6717–6736. doi:10.5194/acp-19-6717-2019

Wang, X., & Zhang, R. (2020), Effects of atmospheric circulations on the interannual variationin $PM_{2.5}$ concentrations over the Beijing–Tianjin–Hebei region in 2013–2018, *Atmospheric Chemistry and Physics*, *20*, 7667–7682. doi:10.5194/acp-20-7667-2020

Wang, Q., Fang, J., Shi, W., & Dong, X. (2020), Distribution characteristics and policy-related improvements of $PM_{2.5}$ and its components in six Chinese cities, *Environmental Pollution*, 266. doi:10.1016/j.envpol.2020.115299

Yan, Y., Zhou, Y., Kong, S., Lin, J., Wu, J., Zheng, H., Zhang, Z., Bai., Y, Ling, Z., Liu, D., & Zhao, T. (2020) Effectiveness of emission control to reduce $PM_{2.5}$ pollution of Central China during winter haze episodes under various potential synoptic controls. *Atmospheric Chemistry and Physics*. doi:10.5194/acp-2020-920

Yu, C., Zhao, T., Bai, Y., Zhang, L., Kong, S., Yu, X., He, J., Cui, C., Yang, J., You, Y., Ma, G., Wu, M., & Chang, J. (2020), Heavy air pollution with a unique "non-stagnant" atmospheric boundary layer in the Yangtze River middle basin aggravated by regional transport of $PM_{2.5}$ over China, *Atmospheric Chemistry and Physics*, *20*, 7217-7230. doi: 10.5194/acp-20-7217-2020

Zhang, H., Yuan, H., Liu, X., Yu, J., & Jiao, Y. (2018), Impact of synoptic weatherpatterns on 24 h-average $PM_{2.5}$ concentrations in the North China Plain during 20132-017, *Science of the Total Environment*, *627*, 200-210. doi: 10.1016/j.scitotenv.2018.01.248

Zhang, J., Zhu, T., Zhang, Q., Li, C., Shu, H., Ying, Y., Dai, Z, Wang, X., Liu, X., Liang, A, Shen, H., & Yi, B. (2012), The impact of circulation patterns on regional transport pathways and air quality over Beijing and its surroundings. *Atmospheric Chemistry and Physics*, 12, 5031–5053, doi: 10.5194/acp-12-5031-2012

Zhang, K., Zhao, C., Fan, H., Yang, Y., & Sun, Y. (2019), Toward Understanding the Differences of $PM_{2.5}$ Characteristics Among Five China Urban Cities. *Asia-Pacific Journal of Atmospheric Sciences*, 1–10, doi:10.1007/S13143-019-00125-W

Zhang, Q., Zheng, Y., Tong, D., Shao, M., Wang, S., Zhang, Y., Xu, X., Wang, J., He, H., & Liu, W. (2019), Drivers of improved $PM_{2.5}$ air quality in China from 2013 to 2017. *Proceedings of the National Academy of Sciences*, 116, 24463–24469. doi:10.1073/pnas.1907956116

Zhang, Q., Quan, J., Tie, X., Li, X., Liu, Q., Gao, Y., & Zhao, D. (2015), Effects of meteorology and secondary particle formation on visibility during heavy haze events in Beijing, China. *Science of the Total Environment*, *502*, 578–584, doi:10.1016/j.scitotenv.2014.09.079

Zhang, Q., Song, Y., Li, M., & Zheng, B. (2020), Anthropogenic Emissions of SO_2 , NOx , and NH_3 in China, in: Atmospheric Reactive Nitrogen in China: Emission, Deposition and Environmental Impacts, edited by: Liu, X. and Du, E., *Springer Singapore*, 13–40, doi:10.1007/978-981-13-8514-8_2

Zhang, R., Li, Q., & Zhang, R. (2013), Meteorological conditions for the persistent severe fog and haze event over eastern China in January 2013. *Science China Earth Sciences*, *57*, 26–35. doi:10.1007/s11430-013-4774-3

Zhang, Y., Ding, A., Mao, H., Nie, W., Zhou, D., Liu, L., Huang, X., & Fu, C. (2016), Impact of synoptic weather patterns and inter-decadal climate variability on air quality in the North China Plain during 1980-2013. *Atmospheric Environment*, *124*, 119–128. doi: 10.1016/j.atmosenv.2015.05.063

Zhou, X., Bei, N., Liu, H., Cao, J., Xing, L., Lei, W., Molina, L.T., & Li, G. (2017), Aerosol effects on the development of cumulus clouds over the Tibetan Plateau. *Atmospheric Chemistry and Physics*, *17*(12), 7423–7434. doi: 10.5194/acp-17-7423-2017

Zhu, W., Xu, X., Zheng, J., Yan, P., Wang, Y., & Cai, W. (2018), The characteristics of abnormal wintertime pollution events in the Jing-Jin-Ji region and its relationships with meteorological factors, *Science of the Total Environment*, *626*, 887–898. doi:10.1016/j.scitotenv.2018.01.083

Zhu, Y., Zhao T., Bai, Y., Xu, J., Sun, X., Hu, W., Chang J., Yang J., & Zhu, C. (2021), Characteristics of Atmospheric Particulate Matter Pollution and the Unique Wind and Underlying Surface Impact in the Twain-Hu Basin in Winter. *Environmental. Science* (in Chinese). doi:10.13227/j.hjkx.202103050.

Zhong, J., Zhang, X., Wang, Y., Wang, J., Shen, X., Zhang, H., Wang, T., Xie, Z., Liu, C., Zhang, H., Zhao, T., Sun, J., Fan, S., Gao, Z., Li, Y., & Wang, L. (2019), The two-way feedback mechanism between unfavorable meteorological conditions and cumulative aerosol pollution in various haze regions of China. *Atmospheric Chemistry and Physics*, *19*(5), 3287-3306. doi: 10.5194/acp-19-3287-2019

Zhong, Q., Ma, J., Shen, G., Shen, H., Zhu, X., Yun, X., Meng, W., Cheng, H., Liu, J., Li, B., Wang, X., Zeng, E. Y., Guan, D., & Tao, S. (2018), Distinguishing Emission-Associated Ambient Air $PM_{2.5}$ Concentrations and Meteorological Factor-Induced Fluctuations. *Environmental Science & Technology*, *52*. doi:10.1021/acs.est.8b02685

Zong, L., Yang, Y., Gao, M., Wang, H., Wang, P., Zhang, H., Wang, L., Ning, G., Liu, C., Li, Y., & Gao., Z. (2021), Large-scale synoptic drivers of co-occurring summertime ozone and $PM_{2.5}$ pollution in eastern China. *Atmospheric Chemistry and Physics*, *21*(11), 9105-9124. doi:10.5194/acp-21-9105-2021

JGR-Atmospheres

Supporting Information for

Regulation of synoptic circulation in regional $PM_{2.5}$ transport for heavy air pollution: study of 5-year observation over central China

Weiyang Hu[1], Tianliang Zhao[1], Yongqing Bai[2], Shaofei Kong[3], Lijuan Shen[1], Jie Xiong[2], Yue Zhou[2], Yao Gu[1], Junnan Shi[4], Huang Zheng[3], and Xiaoyun Sun[1]

[1]Climate and Weather Disasters Collaborative Innovation Center, Key Laboratory for Aerosol-Cloud-Precipitation of China Meteorological Administration, PREMIC, Nanjing University of Information Science &Technology, Nanjing, 210044, China.

[2]Institute of Heavy Rain, China Meteorological Administration, Wuhan, 430205, China.

[3]Department of Atmospheric Sciences, School of Environmental Studies, China University of Geosciences (Wuhan), Wuhan, 430074, China.

[4]Taishan meteorological station of Shandong province, Taishan, 271000, China

Correspondence: tlzhao@nuist.edu.cn (T.L. Zhao) and 2007byq@163.com

Contents of this file

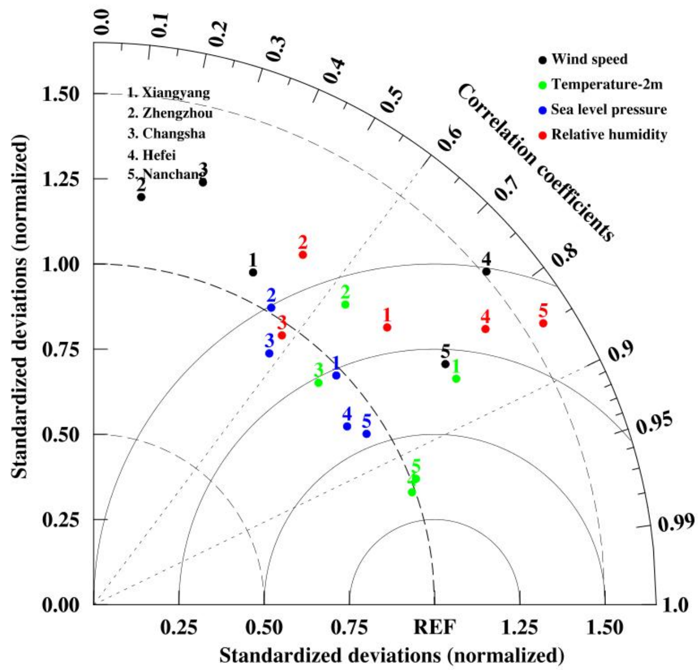

Figure S1. Comparisons in Taylor plots (Taylor, 2001) manifesting the standard deviations and correlation coefficients between the simulated and observed meteorological elements including 10-m wind speed, 2-m air temperature, air pressure and relative humidity at 5 urban sites (Xiangyang, Zhengzhou, Changsha, Hefei, and Nanchang) over the THB.

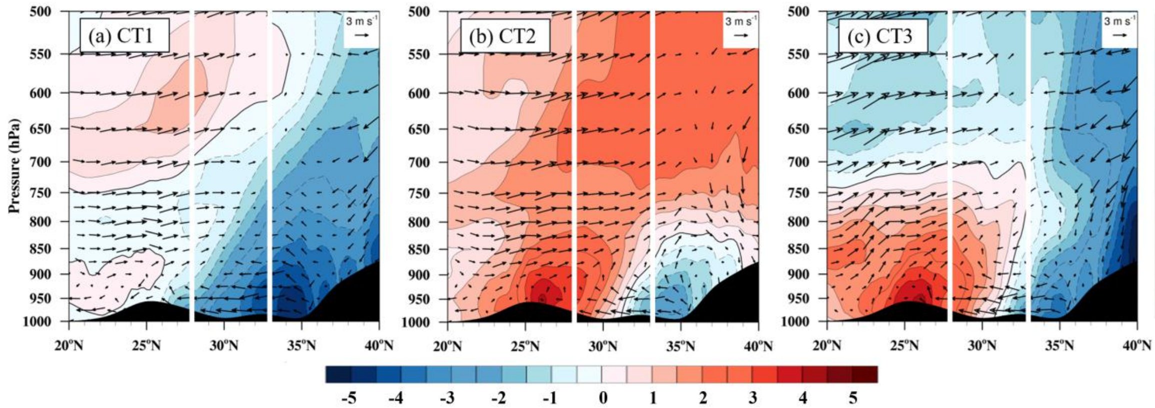

Figure S2. Vertical cross sections of air temperature anomalies (color contours, ℃) and wind vectors for three synoptic circulation types (a) CT1, (b) CT2, (c) CT3 over CEC. The vertical wind components were multiplied by 20 to better display vertical circulations. With the white frames marking atmospheric columns over the THB in central China.

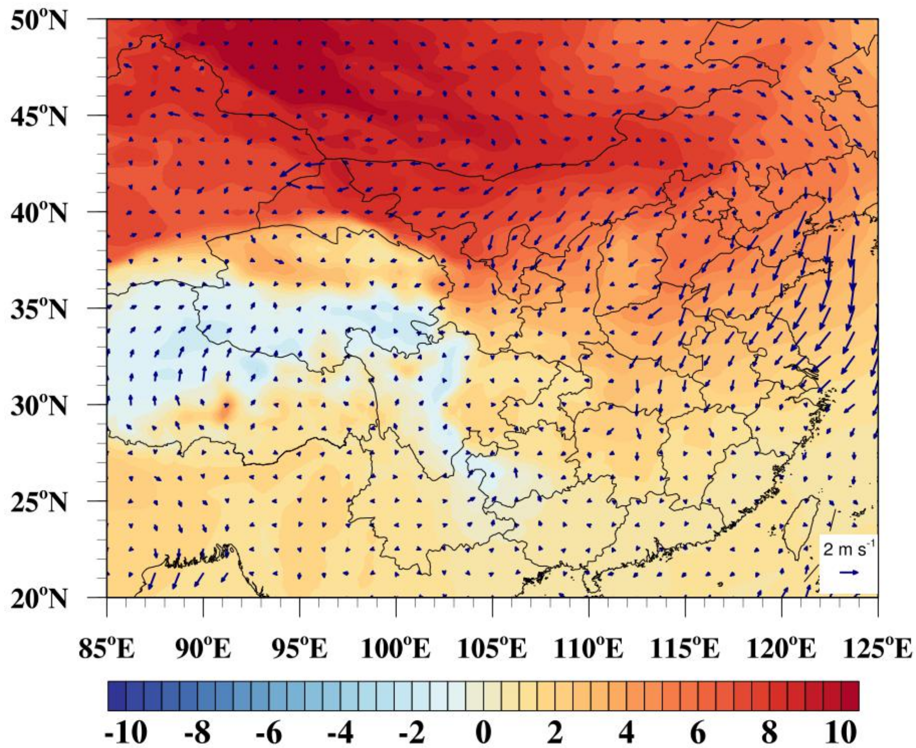

Figure S3. Distribution of anomalies of sea level pressure (unit: hPa) and 10-m wind vectors (unit: m s $^{-1}$) in CT1 relatively to the wintertime averages over 2015–2019.

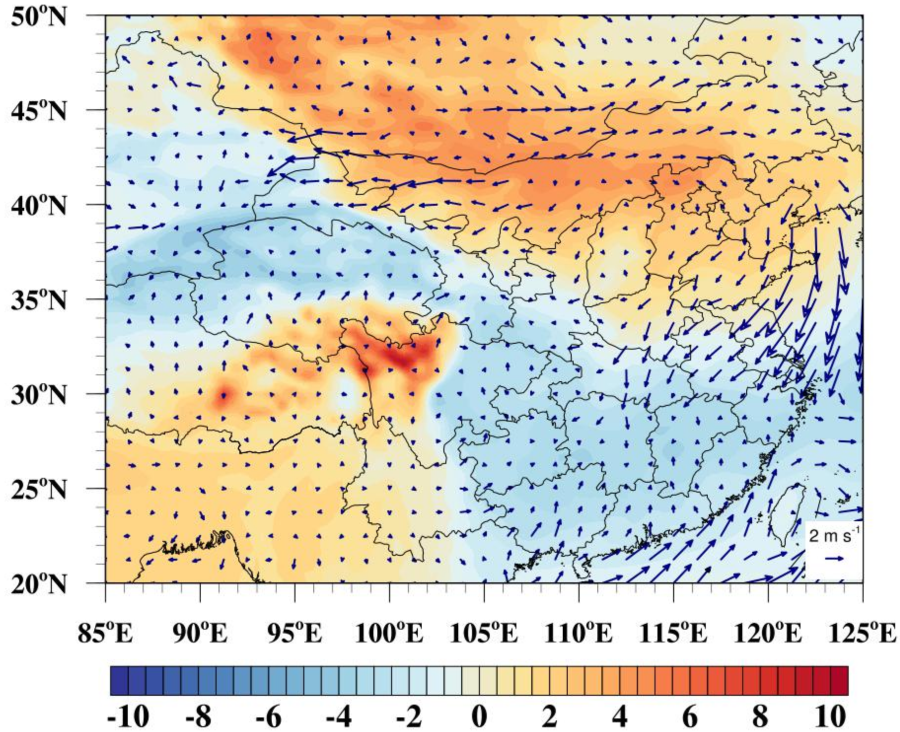

Figure S4. Distribution of anomalies of sea level pressure (unit: hPa) and 10-m wind vectors (unit: m s $^{-1}$) in CT3 relatively to the wintertime averages over 2015–2019.

Table S1 WRF model configurations.

Regions	CEC
Domain size	265 × 541 grid cells; 200 × 283 grid cells
Horizontal resolution	30 km; 10 km
Vertical resolution	33 sigma levels
Microphysics	Lin scheme
Longwave radiation	RRTM scheme
Shortwave radiation	Goddard shortwave scheme
Surface layer	MM5 similarity surface layer
Land-surface	the unified Noah land surface model
Urban canopy model	Single-layer UCM scheme
Boundary layer	YSU boundary layer scheme
Cumulus	Grell 3-D ensemble scheme

Photolysis	Fast-J
Spin-up time	48 h
Simulation period	Wintertime over 2015 to 2019

Table S2 Statistics of heavy air pollution days over the THB during 2015–2019.

Date (YYYYMMDD)	Number of cities with heavy air pollution	Average $PM_{2.5}$ concentrations ($\mu g\ m^{-3}$)	Maximum $PM_{2.5}$ concentrations ($\mu g\ m^{-3}$)
20151211	9	156	277
20151212	11	179	264
20151223	5	133	190
20151224	3	115	178
20151225	9	164	281
20151230	4	128	169
20160102	4	131	206
20160104	8	163	342
20160105	4	129	229
20160111	6	133	215
20160118	8	154	235
20160130	3	99	208
20160208	12	196	312
20160306	3	99	183
20161115	4	114	261
20161209	3	122	176
20161220	4	125	417
20170102	7	138	185
20170103	8	154	213
20170104	13	179	229
20170128	14	221	449
20170217	4	130	165
20170306	6	139	216
20170307	6	137	203
20171204	4	124	278
20171205	6	141	185
20171229	3	119	279
20171230	3	118	170
20180102	3	104	207
20180119	10	171	307

20180120	5	126	228
20180216	5	133	190
20181130	7	150	237
20181201	10	176	269
20181202	5	129	203
20190105	7	154	279
20190106	12	175	324
20190107	8	159	287
20190108	8	152	270
20190126	5	125	190
20190128	3	119	154
20190129	3	120	186
20190130	4	113	194
20190205	10	158	252
20191214	4	132	187
20191215	4	122	211

Table S3 Statistics of 30-day HPEs dominated by regional $PM_{2.5}$ transport with corresponding transport contribution rates to the THB' s regional $PM_{2.5}$ concentrations.

ID	Date (YYYYMMDD)	Contribution rates (%)
1	20151211	66.90
2	20151212	70.90
3	20151223	70.60
4	20151224	70.30
5	20160104	75.00
6	20160105	80.30
7	20160111	63.20
8	20160118	73.70
9	20160130	78.90
10	20161115	75.00
11	20161209	40.70
12	20161220	60.90
13	20170103	44.70
14	20170217	62.20
15	20170306	61.50
16	20170307	53.40
17	20171204	69.70
18	20171205	56.40
19	20171229	30.10
20	20181130	50.00

21	20190105	76.80
22	20190106	45.60
23	20190107	36.60
24	20190108	77.60
25	20190126	84.90
26	20190128	50.00
27	20190129	59.80
28	20190130	28.90
29	20191214	38.30
30	20191215	52.40
average	-	60.20

Table S4 Statistics of three types of synoptic circulation with the date (YearMonthDay) during wintertime over 2015–2019, and CT indicated by the numbers 1, 2 or 3 respectively for three synoptic circulation types CT1, CT2 or CT3.

Date (YYYYMMDD)	CT	Date (YYYYMMDD)	CT
20151211	2	20170307	1
20151212	2	20171204	1
20151223	1	20171205	1
20151224	2	20171229	1
20160104	3	20181130	2
20160105	3	20190105	1
20160111	1	20190106	1
20160118	3	20190107	1
20160130	1	20190108	2
20161115	3	20190126	1
20161209	2	20190128	1
20161220	1	20190129	2
20170103	2	20190130	2
20170217	2	20191214	2
20170306	1	20191215	2

Table S5 Regional averages of meteorological variables 2-m air temperature (T), relative humidity (RH), air pressure (P) and 10-m wind speed (WS) as well as $PM_{2.5}$ concentrations over the THB under three synoptic circulation types CT1, CT2 and CT3.

Synoptic types	T (℃)	RH (%)	P (hPa)	WS (m s^{-1})	$PM_{2.5}$ (μg m^{-3})
CT1	5.2	77.5	1027.6	2.6	143.5

CT2	7.4	77.9	1025.5	2.7	154.9
CT3	5.6	83.3	1024.6	3.1	152.6

Reference

Taylor, K. E. (2001). Summarizing multiple aspects of model performance in a single diagram. *Journal of Geophysical Research-Atmosphere*, *106*, 7183 – 7192. doi: 10.1029/2000JD900719